General Disclaimer

One or more of the Following Statements may affect this Document

- This document has been reproduced from the best copy furnished by the organizational source. It is being released in the interest of making available as much information as possible.

- This document may contain data, which exceeds the sheet parameters. It was furnished in this condition by the organizational source and is the best copy available.

- This document may contain tone-on-tone or color graphs, charts and/or pictures, which have been reproduced in black and white.

- This document is paginated as submitted by the original source.

- Portions of this document are not fully legible due to the historical nature of some of the material. However, it is the best reproduction available from the original submission.

NASA Technical Memorandum 79001

SUPERSONIC UNSTALLED FLUTTER

J. J. Adamczyk, M. E. Goldstein, and
M. J. Hartmann
Lewis Research Center
Cleveland, Ohio

TECHNICAL PAPER to be presented at the
Fifty-second Meeting of the Propulsion and Energetics Panel
sponsored by AGARD
Cleveland, Ohio, October 23-27, 1978

Prepared for
Agard Propulsion and Energetics Panel
Cleveland, Ohio
October 23-27, 1978

SUPERSONIC UNSTALLED FLUTTER

by J. J. Adamczyk, M. E. Goldstein, and M. J. Hartmann

National Aeronautics and Space Administration
Lewis Research Center
Cleveland, Ohio 44135

SUMMARY

Recently two flutter analyses have been developed at NASA Lewis Research Center to predict the onset of supersonic unstalled flutter of a cascade of two-dimensional airfoils. The first of these analyzes the onset of supersonic flutter at low levels of aerodynamic loading (i.e., backpressure), while the second examines the occurrence of supersonic flutter at moderate levels of aerodynamic loading. Both of these analyses are based on the linearized unsteady inviscid equations of gas dynamics to model the flow field surrounding the cascade. The details of the development of the solution to each of these models have been published. The objective of the present paper is to utilize these analyses in a parametric study to show the effects of cascade geometry, inlet Mach number, and backpressure on the onset of single and multi degree of freedom unstalled supersonic flutter. Several of the results from this study are correlated against experimental qualitative observation to validate the models.

E-9785

INTRODUCTION

The problem of flutter has long plagued the development of high speed compressor fan stages. The solution to this problem is often costly both in terms of time and money. For this reason engine manufacturers as well as government agencies are currently supporting numerous research programs in an attempt to better define regions of flutter instability and solutions to the problem. To date their research activities have uncovered two regions of the operating map of fan stages where flutter can be encountered at high speeds. These regions are shown schematically on the performance map of a typical high speed fan stage in figure 1.

Region I, the zone of moderate to high backpressure supersonic flutter can extend from the stall line of the fan down to its operating line. Experimental evidence of this flutter mode is presented in reference 1.

Region II, the zone of low backpressure supersonic flutter can extend from wide open discharge to slightly below the operating line of the stage. Numerous analytical as well as experimental papers have appeared in the open literature which document the existence of this flutter mode (see refs. 2 to 4). Recently NASA Lewis Research Center has developed analytical analyses for both of these flutter zones. In reference 5 an analyses is developed for the region of moderate to high backpressure flutter, while reference 6 deals with the problem of low backpressure supersonic flutter. Both of these analyses are based on the linearized unsteady inviscid two-dimensional equations of gas dynamics to describe the flow field surrounding an infinite cascade of oscillating thin airfoils in a supersonic stream. The details of the mathematical development of these models will not be presented in the present paper. The objective of the present paper is to utilize these analyses in a parametric study to show the effects of cascade geometry, inlet Mach number, reduced frequency, and backpressure on supersonic flutter. Several of the results from this study are correlated against experimental qualitative observation to validate the models.

MODEL FORMULATION

The present analyses represents an incremental annulus of a fan stage as an infinite two-dimensional cascade of thin airfoils. In both analyses the steady relative flow approaching the cascade is assumed to be supersonic, with a subsonic axial velocity component, and satisfies the Kantrowitz unique incidence relationship. This flow configuration causes the weak oblique leading edge shock wave to propagate upstream of the cascade. At moderate to high pressures it is assumed that the steady pressure rise across the cascade is produced by a system of normal shock waves lying within the cascade passages. Downstream of the shock waves the steady flow is uniform and subsonic. Figure 2 shows a sketch of this steady flow

configuration. As the operating point of the fan at high speeds is moved towards wide open discharge, the system of nearly normal in passage shock waves in the tip region is transformed into a series of weak oblique shock waves (see fig. 2). The flow downstream of these waves is supersonic. Since these waves are weak and the blade sections are thin the steady flow deviates only slightly from a uniform flow at wide open discharge. In both analyses it is assumed that the blade motion results in a small perturbation to a steady two-dimensional base flow solution. At moderate to high backpressure the base flow, as described above, has a normal shock within the cascade passage with a uniform stream approaching and leaving the shock. At wide open discharge the base flow is assumed to be a uniform stream. This assumption according to linear theory uncouples the unsteady flow problem from its steady state counterpart. The motion of the airfoils in both analyses is restricted to simple harmonic motion in time, at a constant interblade phase angle between adjacent airfoils. The governing equations employed in the analyses are the linearized unsteady two-dimensional inviscid equations for a non-conducting gas. The change of the unsteady flow variables across the in passage shock wave are governed by the first order perturbed Rankine-Hugoniot shock relationships. The solution to both problems was obtained by analytical means the details of which can be found in references 5 and 6. These solutions resulted in accurate and efficient computational algorithms for computing the unsteady aerodynamic loading induced by the cascade motion, including the limiting case of a free stream Mach number of 1.

PARAMETRIC STUDY

The work done by the gas stream on the cascade over a cycle of motion is a direct measurement of the susceptibility of the cascade to flutter. If the sign of the work is negative, the cascade is doing work on the gas stream. Under these conditions any small unsupported motion imparted to the cascade will decay in time, hence the system is stable. If however, the sign of the work is positive the gas stream is doing work on the cascade. If this work is not dissipated by the internal

mechanical damping any small unsupported motion imparted to the cascade will grow in time, causing the system to fail.

For a single degree of freedom pitching or plunging motion the nondimensional work done by the gas stream on an airfoil in the cascade is (see ref. 7)

$$W = \alpha_o \pi \, \mathrm{Im}\{C_M\} \tag{1}$$

for pitching motion and

$$W = h_o \pi \, \mathrm{Im}\{C_L\} \tag{2}$$

for plunging motion, where the symbol $\mathrm{Im}\{\ \}$ denotes the imaginary part of the bracketed quantity. The variables appearing in these two equations are C_M, C_L, α_o, and h_o, which are the complex moment coefficient about the pitching axes, the complex lift coefficient, the amplitude of the pitching oscillation, and the amplitude of the plunging oscillation, respectively. There will be a tendency for single degree of freedom flutter to occur in either the pitching or plunging mode whenever the imaginary part of the complex moment or lift coefficient becomes positive. For two-degree of freedom coupled flutter the nondimensional work done by the gas stream on an airfoil in the cascade is

$$W = -\alpha_o \pi \sin\gamma \, \mathrm{Real}\{C_M\} + h_o \pi \, \mathrm{Im}\{C_L\} + \alpha_o \pi \cos\gamma \, \mathrm{Im}\{C_M\} \tag{3}$$

where the symbol $\mathrm{Real}\{\ \}$ denotes the real part of the complex bracketed quantity and γ is the phase angle at an instant in time between the pitching and plunging motion of an airfoil. Unlike single degree of flutter whose onset is independent of the amplitude of the airfoil motion the onset of coupled flutter as shown by equation (3) is strongly dependent on the ratio of the pitch to plunge amplitudes and their associated phase shift γ.

Computations were performed based on the theory of references 5 and 6 to determine the effect of backpressure, inlet Mach number, reduced frequency, cascade solidity, and stagger angle on the nondimensional aerodynamic work for single degree of freedom pitching and plunging motion and for coupled pitching and plunging motion. These results are shown plotted as a function of the phase angle between two adjacent airfoils (i.e., interblade phase angle) at all times.

SINGLE DEGREE OF FREEDOM FLUTTER

The geometry of the cascade assumed in this study is, solidity 1.3, stagger angle 60° unless otherwise noted. Pitching axis location is assumed to lie at mid-chord. Figures 3 to 7 show graphs of the work per cycle for a cascade undergoing simple harmonic pitching motion at moderate to high backpressures. The in passage normal shock wave is assumed to lie slightly upstream of the passage entrance. Results are shown in figures 3 to 5 for inlet Mach numbers of 1.2, 1.4, and 1.6, respectively. The parameter varied in each of these figures is the reduced frequency based on semichord from a value of 0.25 to 1.0. Recalling that positive work per cycle implies instability provided the effect of mechanical damping is neglected, figures 3 to 5 show that for Mach numbers between 1.2 and 1.6 single degree of freedom pitching (i.e., torsional) flutter can exist for reduced frequencies less than 0.25 at moderate to high backpressures. At Mach numbers above 1.2 this mode of flutter exists for reduced frequencies above 0.25 but ceases to exist at reduced frequencies greater than 0.5. The effects of cascade solidity and stagger angle on torsional flutter at moderate to high backpressures are shown in figures 6 and 7. These results were computed based on solidities of 1.2 and 1.4 and stagger angles of 50° and 70°. The reduced frequency and inlet Mach number were held constant at 0.5 and 1.4. Although figures 6 and 7 show no region of instability they do show that reducing the solidity and decreasing the stagger angle have a slight stabilizing effect on single degree of freedom torsional flutter at moderate to high backpressures.

The nondimensional work per cycle for a cascade pitching about mid-chord at low backpressures is shown in figures 8 to 12. The cascade geometry assumed in the computation of these results is identical to that assumed for the previous results unless otherwise noted. Figures 8 to 10 show the effect of Mach number and reduced frequency. From these results it appears that single degree of freedom torsional flutter will not exist at low backpressures at reduced frequencies in excess of 0.50. This reduced frequency limit is greater than the corresponding limit

established from the previous set of results for moderate to high backpressure cascade operation. This implies that a cascade operating with a finite backpressure across it will be less susceptible to torsional flutter than a cascade operating at low back pressures. This backpressurizing phenomenon has been observed in fans where it causes the torsional flutter boundary to bend back as the pressure ratio across the fan is raised (see fig. 1). The effects of cascade solidity and stagger angle on the work per cycle for torsional oscillation at low backpressures are shown in figures 11 and 12. The values of the parameters used in these computations are identical to those used previously in computing the results in figures 6 and 7. These results like their counterparts for moderate to high backpressure show that reducing the stagger angle and reducing the cascade solidity have a slight stabilizing effect on torsional flutter at low backpressures.

The work per cycle for a cascade undergoing simple harmonic plunging motion at moderate to high backpressures is shown in figures 13 to 17. Figures 13 to 15 show the effects of reduced frequency and Mach number. These results imply that the work per cycle will remain negative over all values of interblade phase angle provided the reduced frequency is slightly greater than 0.20 for inlet Mach numbers up to 1.6. As the inlet Mach number is reduced from 1.6 the transition reduced frequency decreases to approximately 0.15 at Mach number 1.2. The effects of solidity and stagger angle on the work per cycle are shown in figures 16 and 17. Increasing the solidity slightly enhances the stability of the system, while increasing the stagger has a destabilizing effect.

The results for plunging motion at low backpressure are not presented because they showed that the work per cycle always remained negative. Thus the theory of reference 6 predicts that flutter in a pure plunging mode cannot occur at low backpressures. However, the results presented in figures 13 to 17 which were based on the theory of reference 5 show that single degree of freedom bending flutter can occur at moderate to high backpressures. Thus it can be concluded that backpressuring tends to induce bending flutter. Experimental evidence to support this observation is provided in reference 1.

COUPLED FLUTTER

Carta (ref. 8) showed the existence of coupled flutter in compressor rotors. Unlike coupled flutter in fixed wing aircraft where the coupling between the bending and torsional mode is due to the aerodynamic forces, the coupling in compressor rotors is caused by mechanical restraining forces associated with part span shrouds and flexible disks. Carta in his analysis assumed the motion of the rotor disk to be

$$S = Ae^{-i\left(\omega t - \frac{2\pi m}{N}\frac{r}{p}\right)}$$

where A is the amplitude of the motion, t is time, ω is the circular frequency, n is an integer, N is the number of rotor blades, p is the pitch chord ratio, and r the peripherial distance around the wheel. If the rotor blades are rigidly fixed to the deforming disk the plunging and pitching amplitude of a blade section at a given radial location are

$$h_o = A \cos \delta$$

$$\alpha_o = \frac{2\pi mA}{Np} e^{i\pi/2}$$

respectively, where δ is the local stagger angle of the blade sections. The nondimensional aerodynamic work per cycle associated with this motion is

$$W = A\pi \cos \delta \left\{ \text{Im } C_L - \frac{2\pi m}{pN \cos \delta} \text{ Real } C_M \right\}$$

where the integer n can take on both positive and negative values corresponding to either a backward or forward traveling wave along the disk rim. The lift and moment coefficients appearing in this equation are to be evaluated at an interblade phase angle of

$$\sigma = \frac{2\pi m}{N}$$

Computations were performed to assess the influence of the twist bend coupling ratio

$$\epsilon = \frac{2\pi m}{Np \cos \delta}$$

inlet Mach number and reduced frequency on the aerodynamic work per cycle at low and high backpressures. The results for moderate to high backpressures are shown plotted as a function of the harmonic number n for specified values of reduced frequency and inlet Mach number in figures 18 to 20. The cascade solidity and stagger angle are 1.3 and 60°, respectively. These results show that for n negative and large the gas stream is supplying energy to the cascade, while for positive values of n the energy flow is generally from the cascade to the gas stream. Hence, the vibrational waves traveling in the direction of rotation appear to be less stable than those traveling in the opposite direction. For small absolute values of n and for reduced frequencies greater than 0.25 the work per cycle remains negative for Mach numbers greater than 1.2. Since the twist bend coupling parameter ϵ is directly proportional to n it is seen that an effective means of suppressing coupled flutter is by mechanically controlling the ratio of twist to bend in the lower order vibrational modes. These results also show that increasing reduced frequency has a stabilizing effect on coupled flutter but not to the extent it does for single degree of freedom flutter.

The effect of lowering the backpressure across the cascade on the work per cycle is shown in figures 21 to 23. The trends of these results are quite similar to those for moderate to high backpressure. Increasing reduced frequency and limiting the ratio of twist bend coupling suppresses coupled flutter at low backpressure, as it did at high to moderate backpressures. From these results it appears that proper choice of these two parameters can prevent coupled flutter from occurring over the entire high speed operating angle of a fan or compressor stage.

CONCLUSIONS

The results of numerous calculation based on the theory of references 5 and 6 has been presented to show the effect of inlet Mach number, cascade geometry,

reduced frequency, and backpressure on the susceptibility of a cascade to single- and multi-degree of freedom flutter. It was shown that increasing reduced frequency and backpressure had a stabilizing effect on single degree of freedom torsional flutter. It was also shown that single degree of freedom bending flutter could occur at moderate to high backpressure if the reduced frequency was below 0.25. For a coupled vibrational mode it was shown that the occurrence of flutter could be prevented over the entire high speed operating range of a fan stage by mechanically controlling the ratio of twist bend coupling and reduced frequency. These stability trends are consistent with experimental rig observations.

A detailed experimental verification of the theories of references 5 and 6 in necessary. One suitable approach would be to utilize a high speed wind tunnel with a linear cascade in which the airfoils are driven in a prescribed mode and operated over a range of back pressures. Measured surface pressure distributions could then be correlated against predicted results to establish the model validity or the need for additional model refinements.

REFERENCES

1. Ruggeri, R. S.; and Benser, W. A.: Performance of Highly Loaded Two-Stage Axial-Flow Fan. NASA TM X-3076, 1974.

2. Kurosaka, M.: On the Unsteady Supersonic Cascade with a Subsonic Leading Edge - An Exact First Order Theory: Parts 1 and 2. J. Eng. Power, vol. 96, no. 1, Jan. 1974, pp. 13-31.

3. Verdon, J. M.: Further Developments in the Aerodynamic Analysis of Unsteady Supersonic Cascades Parts 1 and 2. ASME Paper 77-GT-44 and 77-GT-45, Mar. 1977.

4. Snyder, L. E.; and Commerford, G. L.: Supersonic Unstalled Flutter in Fan Rotors; Analytical Experimental Results. J. Eng. Power, vol. 96, no. 4, Oct. 1974, pp. 379-386.

5. Goldstein, M. E.; Braun, W.; and Adamczyk, J. J.: Unsteady Flow in a Supersonic Cascade With Strong In-Passage Shocks. J. Fluid Mech., vol. 83, part III, 1977, pp. 569-604.

6. Adamczyk, J. J.; and Goldstein, M. E.: Unsteady Flow in a Supersonic Cascade with Subsonic Leading Edge Locus. To be published in the AIAA Journal.

7. Fung, Yuan-cheng: An Introduction to the Theory of Elasticity. Wiley, New York, 1955, pp. 166-168.

8. Carta, F. O.: Coupled Blade-Disk-Shroud Flutter Instabilities in Turbojet Engine Rotors. J. Eng. Power, vol. 89, no. 3, July 1967, pp. 419-426.

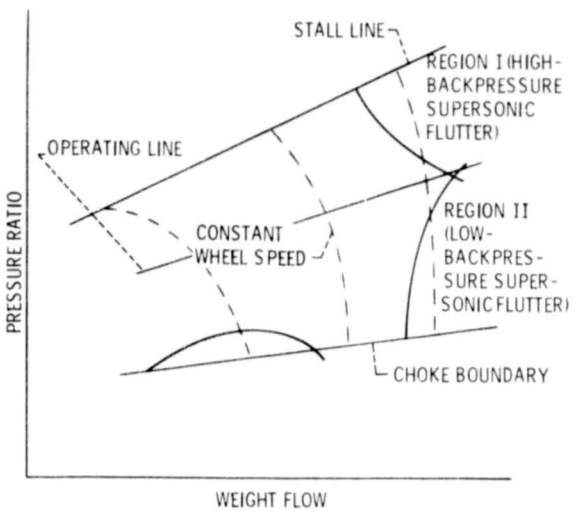

Figure 1. - Compressor performance and stability map.

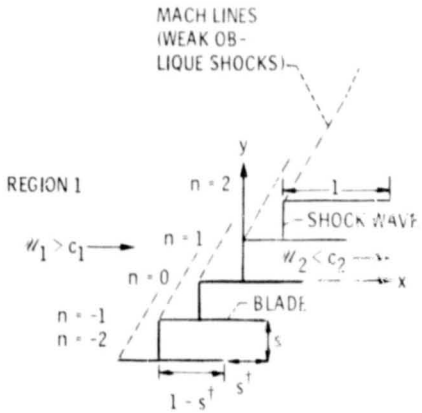

(a) FLOW CONFIGURATION AT MODERATE TO HIGH BACK-PRESSURES.

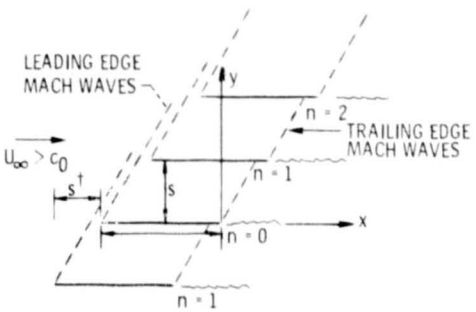

(b) FLOW CONFIGURATION AT LOW BACKPRESSURES.

Figure 2.

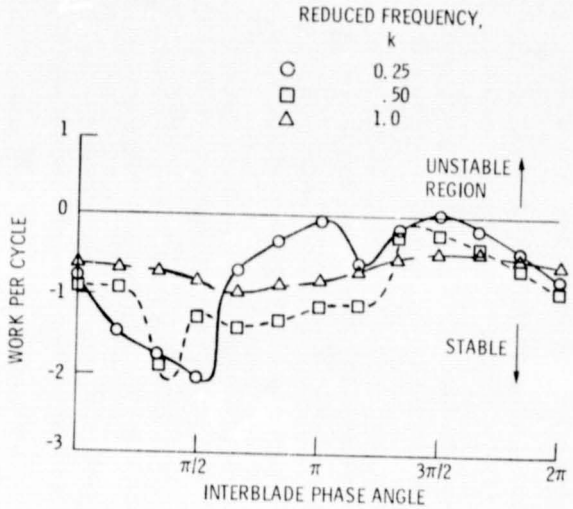

Figure 3. - Work per cycle for pitching motion about mid-chord at moderate backpressure (Mach no. 1.2).

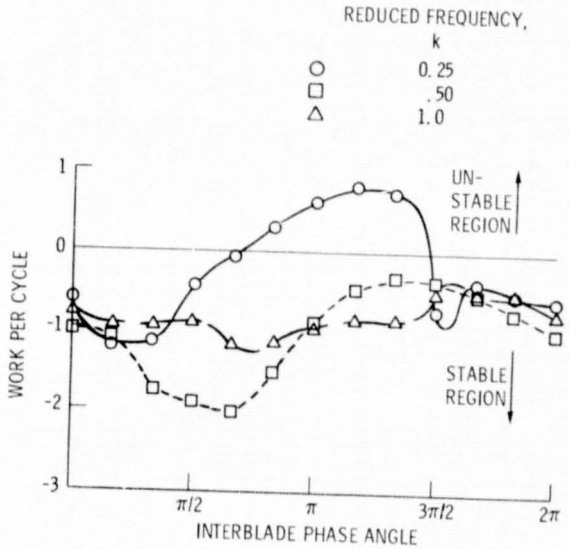

Figure 4. - Work per cycle for pitching motion about mid-chord at moderate backpressure (Mach no. 1.4).

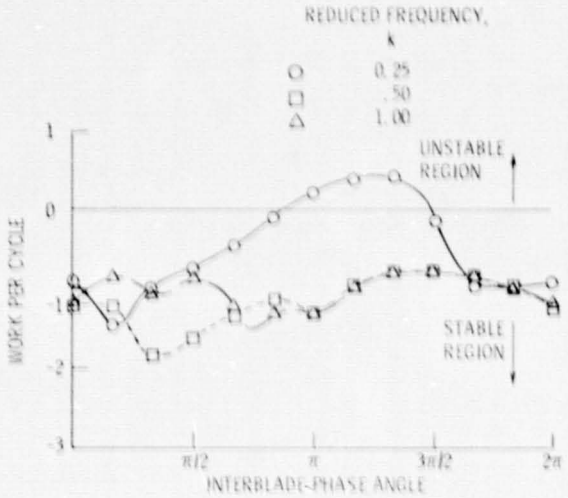

Figure 5. - Work per cycle for pitching motion about mid-chord at moderate backpressure (Mach no. 1.6).

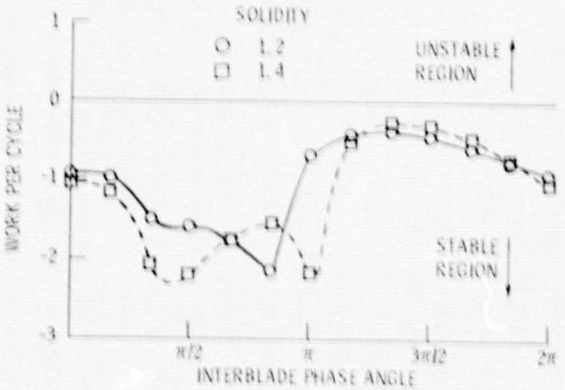

Figure 6. - The effect of solidity on the work per cycle for pitching motion at moderate backpressure.

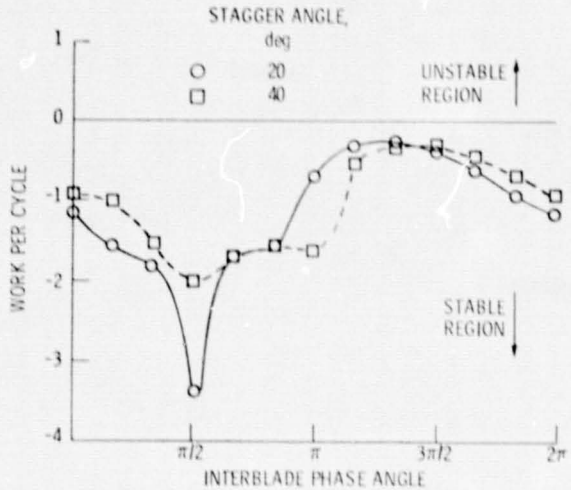

Figure 7. - The effect of stagger angle on the work per cycle for pitching motion at moderate backpressure.

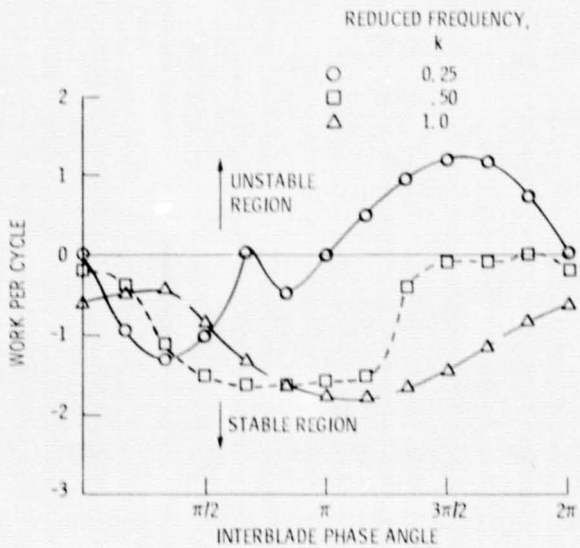

Figure 8. - Work per cycle for pitching motion about mid-chord at low backpressure (Mach no. 1.2).

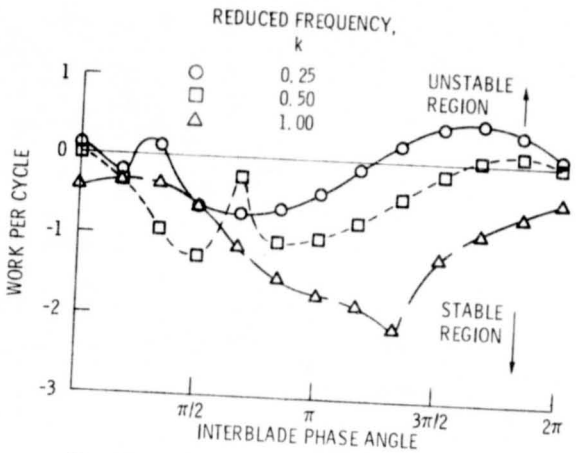

Figure 9. - Work per cycle for pitching motion about mid-chord at low backpressure (Mach no. 1.4).

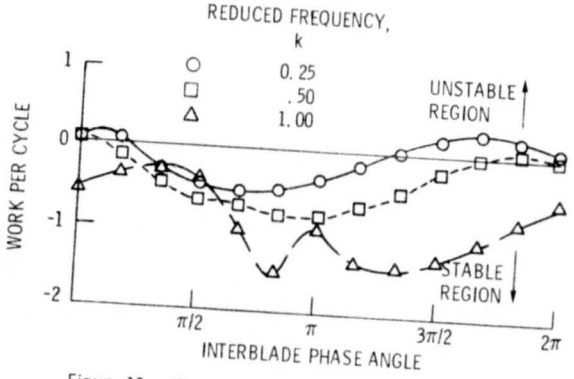

Figure 10. - Work per cycle for pitching motion about mid-chord at low backpressure (Mach no. 1.6).

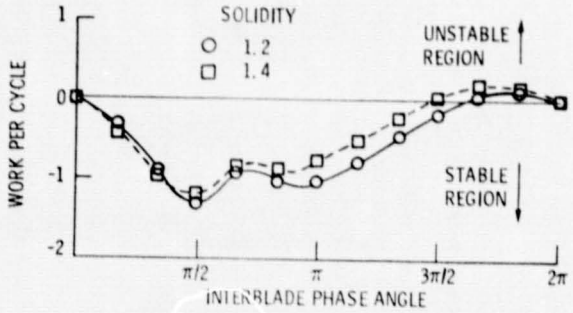

Figure 11. - The effect of solidity on the work per cycle for pitching motion at low backpressure.

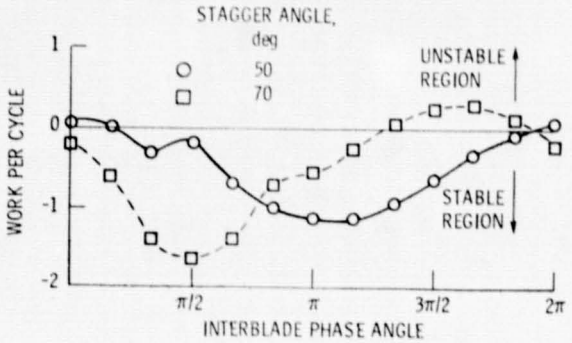

Figure 12. - The effect of stagger angle on the work per cycle for pitching motion at low backpressure.

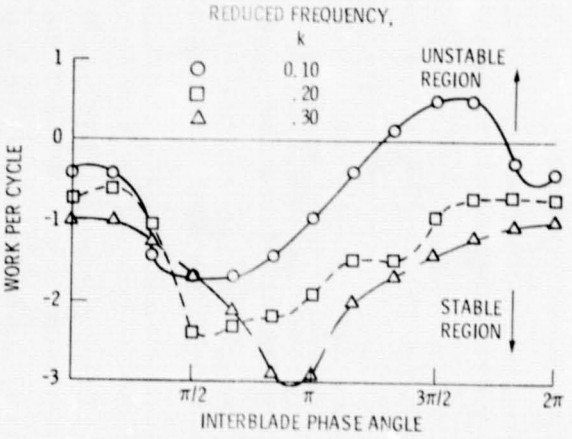

Figure 13. - Work per cycle for plunging motion at moderate backpressure (Mach no. 1.2).

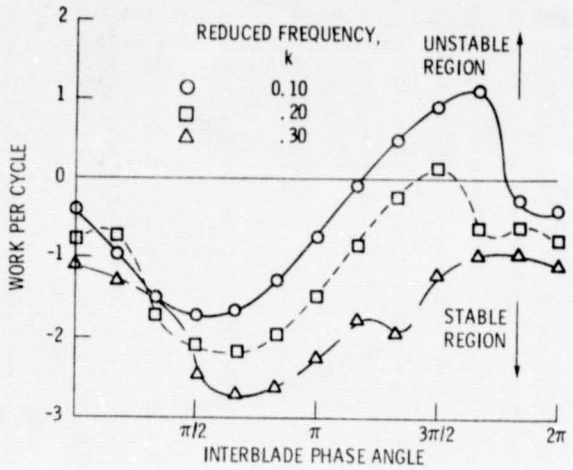

Figure 14. - Work per cycle for plunging motion at moderate backpressure (Mach no. 1.4).

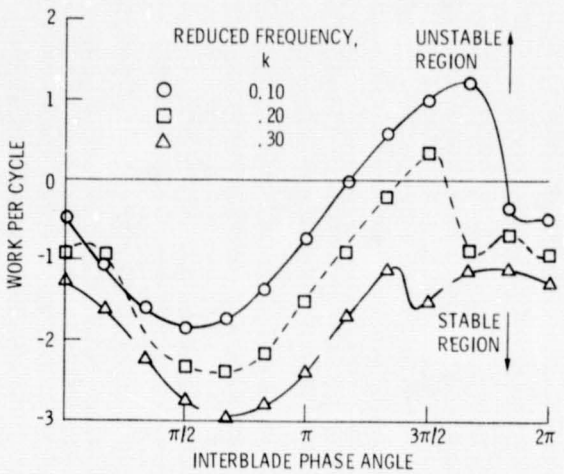

Figure 15. - Work per cycle for plunging motion at moderate backpressure (Mach no. 1.6).

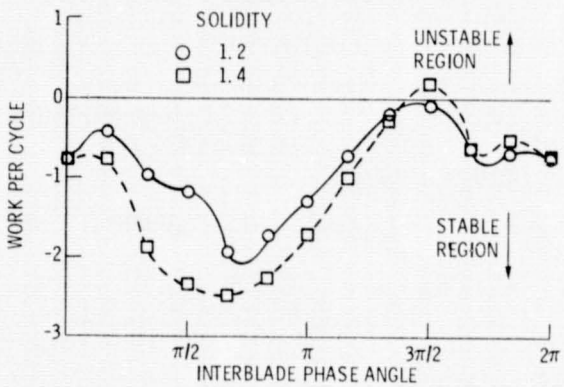

Figure 16. - The effect of solidity on the work per cycle for plunging motion at moderate backpressure.

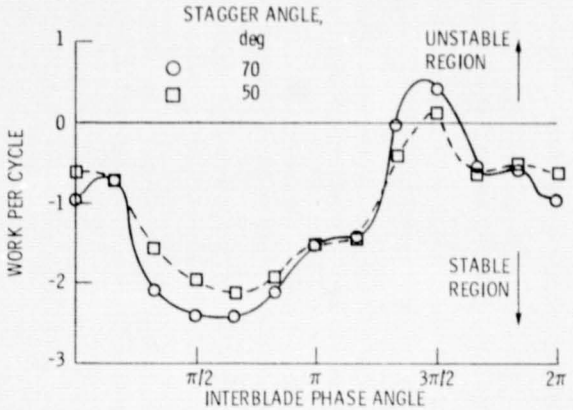

Figure 17. - The effect of stagger angle on the work per cycle at moderate backpressure.

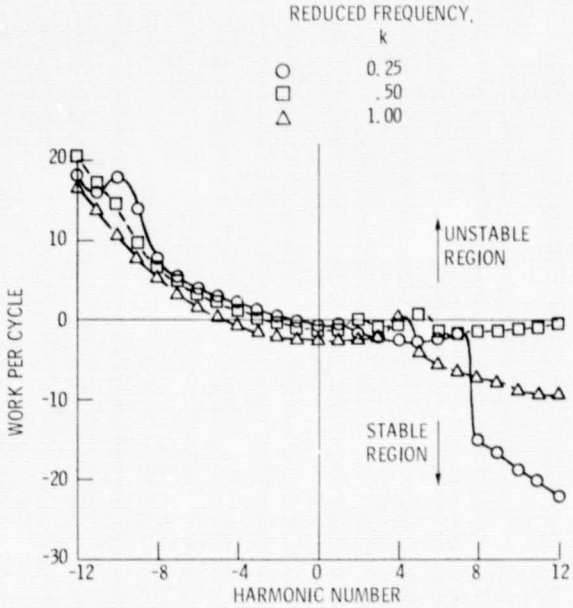

Figure 18. - Work per cycle for coupled motion at moderate backpressure (Mach no. 1.2).

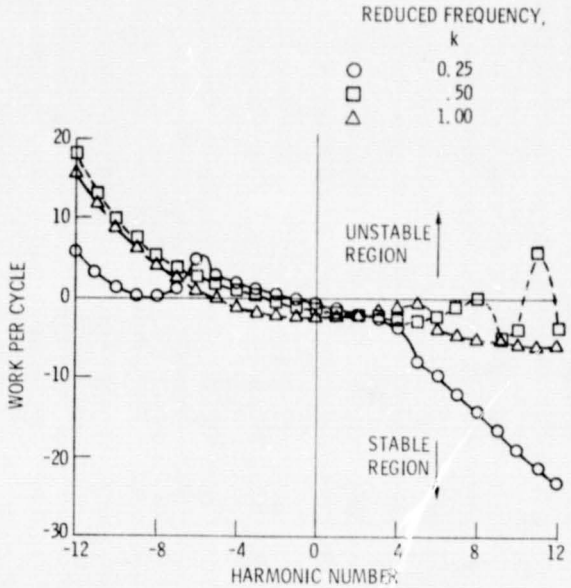

Figure 19. - Work per cycle for coupled flutter at moderate backpressure (Mach no. 1.4).

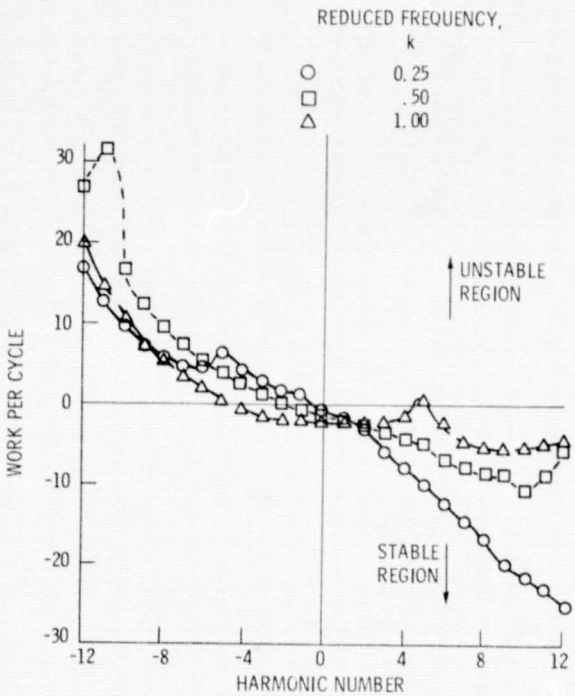

Figure 20. - Work per cycle for coupled motion at moderate backpressure (Mach no. 1.6).

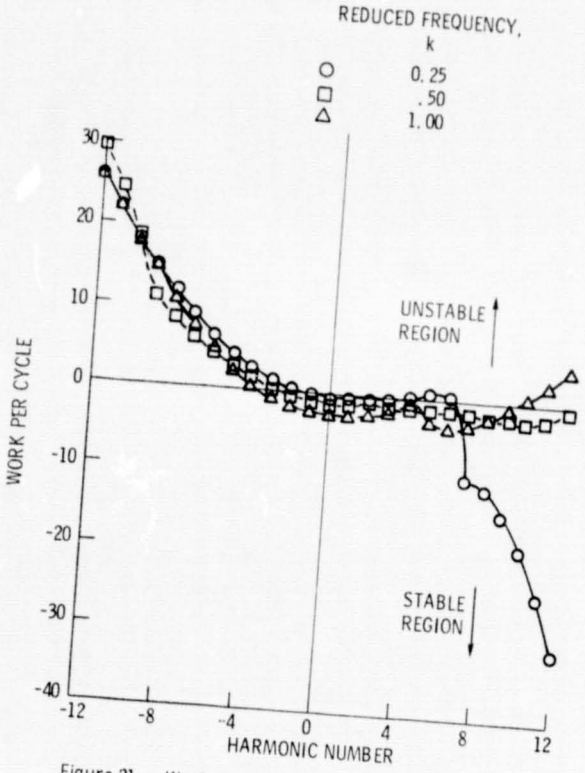

Figure 21. - Work per cycle for coupled motion at low back-pressure (Mach no. 1.2).

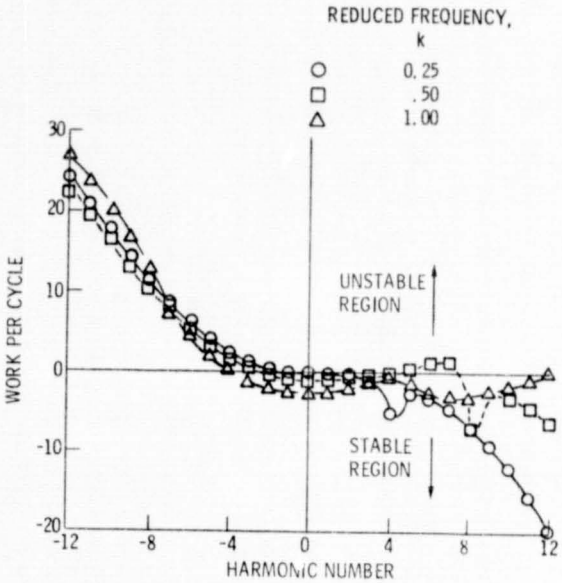

Figure 22. - Work per cycle for coupled motion at low back-pressure (Mach no. 1.4).

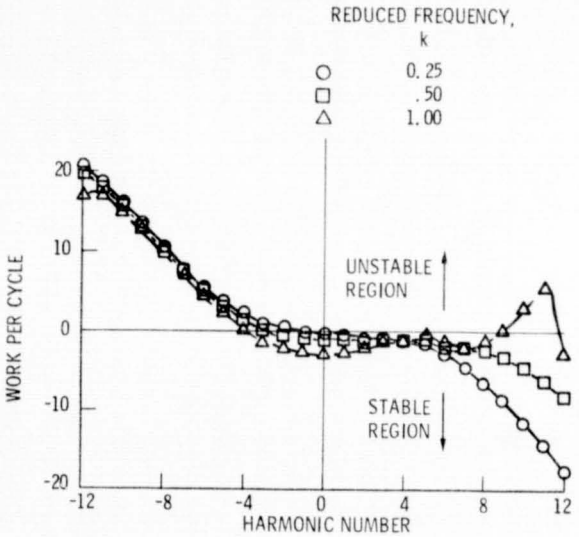

Figure 23. - Work per cycle for coupled motion at low back-pressure (Mach no. 1.6).